

Motion-Aware Generative Frame Interpolation

Guozhen Zhang^{1,2,‡,*} Yuhan Zhu^{1,‡} Yutao Cui² Xiaotong Zhao² Kai Ma² Limin Wang^{1,3,†}

¹State Key Laboratory for Novel Software Technology, Nanjing University

²Platform and Content Group (PCG), Tencent ³Shanghai AI Lab

https://mcg-nju.github.io/MoG_Web/

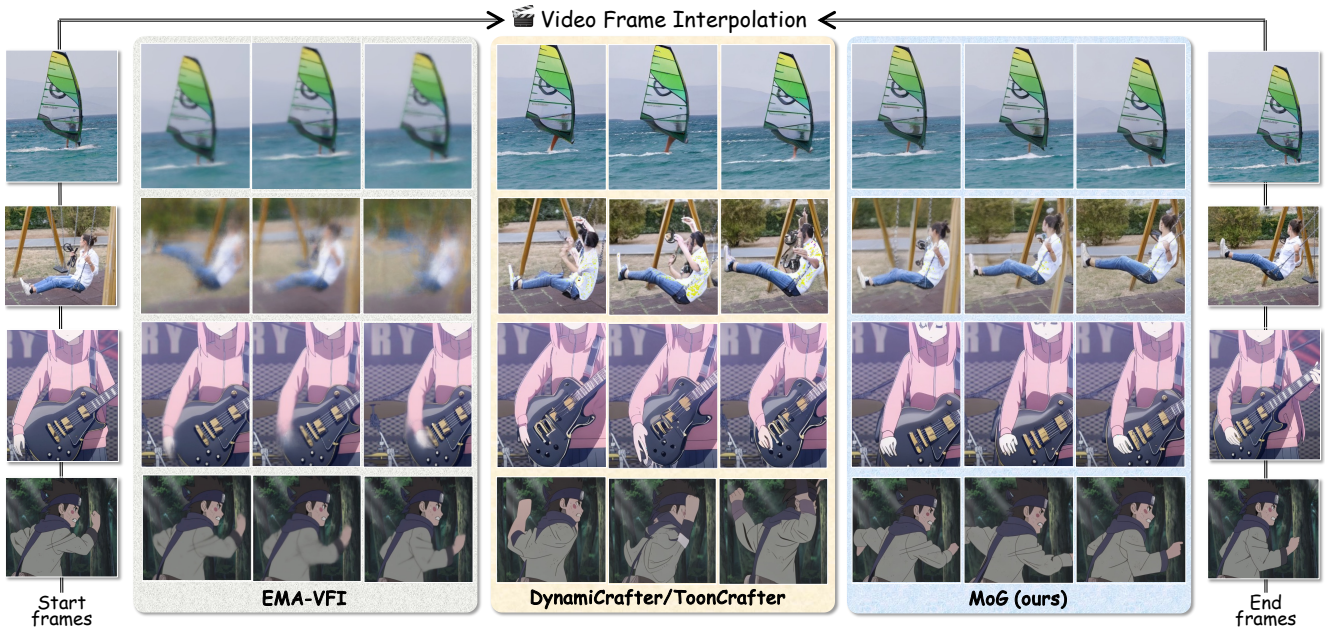


Figure 1. **Examples of frame interpolation in real-world and animation scenes.** Compared to other methods, our approach, MoG, exhibits superior stability in motion and consistency in content relative to the input frames. For optimal viewing, please zoom in.

Abstract

Generative frame interpolation, empowered by large-scale pre-trained video generation models, has demonstrated remarkable advantages in complex scenes. However, existing methods heavily rely on the generative model to independently infer the correspondences between input frames—an ability that is inadequately developed during pre-training. In this work, we propose a novel framework, termed **Motion-aware Generative frame interpolation (MoG)**, to significantly enhance the model’s motion awareness by integrating explicit motion guidance. Specifically we investigate two key questions: **what** can serve as an effective motion guidance, and **how** we can seamlessly embed this guid-

ance into the generative model. For the first question, we reveal that the intermediate flow from flow-based interpolation models could efficiently provide task-oriented motion guidance. Regarding the second, we first obtain guidance-based representations of intermediate frames by warping input frames’ representations using guidance, and then integrate them into the model at both latent and feature levels. To demonstrate the versatility of our method, we train MoG on both real-world and animation datasets. Comprehensive evaluations show that our MoG significantly outperforms the existing methods in both domains, achieving superior video quality and improved fidelity.

1. Introduction

Video Frame Interpolation (VFI), which seeks to synthesize intermediate frames between two input frames, has gar-

*Work is done during internship at Tencent PCG. ‡Equal contribution. †Corresponding author (lmwang@nju.edu.cn).

nered significant attention in recent years due to its capacity for enhancing video frame rates in video post-processing. Flow-based VFI methods [10, 13, 15, 41, 42] predominantly rely on correspondence information through estimating the motion between input frames—termed intermediate flow—to warp information and generate intermediate frames. However, these approaches are primarily optimized for rigid motion scenarios. Consequently, when confronted with complex scenes, the interpolated frames often exhibit pronounced blurring and artifacts, as the results of the flow-based method EMA-VFI [41] shown in Fig. 1.

To overcome these limitations, recent advancements [3, 33–35] have shifted towards leveraging video generation models [2, 35] for frame interpolation, capitalizing on their strong generative capabilities in dynamic scenes. Despite the notable improvements exhibited in complex scenarios [34], current approaches still face a key challenge: they fail to explicitly exploit the dynamics between the two input frames. Instead, *they solely rely on the generative model to infer the correspondences between input frames by itself—an ability that is insufficiently nurtured during the generative pre-training*. Consequently, the videos generated by these methods often suffer from unstable motion and incoherent content to input frames, as shown by *DynamiCrafter* [35] and *ToonCrafter* [34] in Fig. 1.

In this work, we introduce a new framework, **Motion-aware Generative frame interpolation (MoG)**, marking the first explicit incorporation of motion guidance between input frames to enhance the motion awareness of generative models. Our approach significantly alleviates the difficulty of inferring the dynamics between input frames to generate the realistic motion. To achieve this goal, we address two pivotal questions: what can serve as an effective motion guidance, and how to seamlessly and harmlessly integrate this guidance into the generative model.

For the first question, we propose leveraging the intermediate flow from flow-based frame interpolation models [41] as explicit motion guidance. The intermediate flow can be utilized to obtain coarse approximations of intermediate frames under the assumption of rigid motion, which can serve as effective guidance to inspire and stabilize the inference of realistic motion in the generation process. Moreover, compared to direct estimation by pre-trained optical flow models [28, 36, 37], the intermediate flow is task-oriented trained [38], making it inherently more suitable for generating intermediate frames. Flow-based interpolation models also specifically account for occlusion masks [41] between the two input frames, enabling a more accurate aggregation of information into the intermediate frame—something that optical flow often fails to achieve.

To address the second question, we propose a simple yet effective strategy: warping the information from input frames to derive the guidance-based intermediate frame rep-

resentations, which are subsequently integrated into the pre-trained model as explicit motion cues. This integration is performed at both the latent and feature levels, enabling the model to be fully aware of the correspondences between input frames. Specifically, at the latent level, we concatenate a collection of auxiliary latents to the input at each denoising step [8], which includes the latents from the input frames as well as the warped intermediate latents. In terms of feature-level integration, we reuse the pre-trained temporal layers [35] to temporally smooth the warped features, ensuring their alignment within the original feature space, and then incorporate them into the network. Notably, our design requires no additional parameters and achieves improved performance with few fine-tuning steps.

To comprehensively evaluate the versatility of our method, we develop MoG for both the real-world and animation scenes. Furthermore, we meticulously curate two testing datasets, VFIBench-Real and VFIBench-Ani, to assess the performance of each scenes. Experimental results indicate that MoG significantly outperforms the existing generative interpolation models in both qualitative and quantitative aspects. Qualitatively, the videos generated by MoG exhibit enhanced motion stability and greater content consistency, as evidenced in Fig. 1. Quantitatively, MoG demonstrates the obvious improvements in video quality metrics and superior fidelity when compared to ground truth videos. Our contributions are summarized as follows:

- We introduce a new generative frame interpolation framework, MoG, which is the first to incorporate motion guidance to enhance the motion awareness.
- We demonstrate that the intermediate flow from flow-based VFI can effectively serve as a motion guidance, and we design a simple and efficient method to integrate this prior into the network at both the latent and feature levels.
- We validate the effectiveness of MoG in both real-world and animated scenarios, with experimental results showing that MoG significantly outperforms existing open-source generative frame interpolation methods.

2. Related Work

2.1. Flow-based Frame Interpolation

Flow-based video interpolation, explicitly estimating the intermediate flow from the input frames to the intermediate frame, have become dominant in deterministic frame interpolation [17]. It can be broadly categorized into two classes based on how the intermediate optical flow is derived. The first class [1, 9, 12, 18–20] utilized pre-trained optical flow models to obtain the intermediate flow either directly or through refinement. For instance, *SoftSplat* [19] linearly adjusted the bidirectional flow estimated by *PWC-Net* [27] to represent the intermediate flow and employs an improved forward warping to aggregate information. The

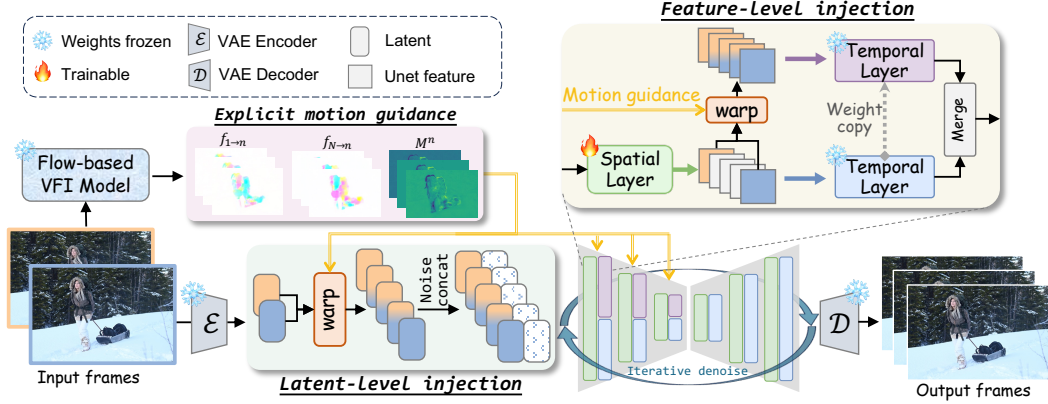


Figure 2. **Overview of MoG.** MoG consists of two parts. First, it extracts the motion guidance of the input frames using a pre-trained flow-based VFI model. Subsequently, this guidance is seamlessly injected into the generative model at both the latent and feature levels.

second class [10, 13–16, 21, 41, 42] modeled the correspondence information of the input frames to directly predict the intermediate flow, offering greater flexibility and task-oriented modeling capacity compared to the first approach. RIFE [10] demonstrated that simple convolutional layers can effectively predict the intermediate flow, achieving impressive efficiency. Similarly, EMA-VFI [41] enhanced the flow prediction by explicitly modeling the dynamics between frames through inter-frame cross-attention. However, both of classes are primarily designed under the assumption of rigid motion scenes. When confronted with complex motion scenarios, they often exhibit significant blurring and artifacts. In our work, we focus on the generative frame interpolation by leveraging the second class of flow-based video frame interpolation (EMA-VFI [41]) to provide explicit motion guidance.

2.2. Generative Frame Interpolation

Recent work has begun to explore the use of large-scale pre-trained video generation models [2, 35], which excel at generating videos in complex dynamic scenes, for the VFI task. Current generative frame interpolation methods can be categorized into two types: the first [3, 33] employed pre-trained generative models to perform image-to-video tasks conditioned on the initial and final frames, subsequently merging the resulting videos to create the final interpolated frame. For example, GI [33] enhanced the motion stability by controlling the consistency of temporal correlations across the two generation processes. The second category [15, 32, 34, 35, 44] focused on fine-tuning video generation models specifically for interpolation, by integrating information from input frames into the model’s architecture and optimizing it for end-to-end interpolation. DynamiCrafter [35] was trained for real-world interpolation, while ToonCrafter [34] was tailored for animated scenes. Although all these methods have demonstrated significant improvements in generating complex scenarios, they do

not explicitly consider the correspondence between input frames, which complicates the motion inference of generative models. In contrast, we are the first to explicitly introduce the correspondence guidance to enhance the motion awareness of generative models and our method achieves superior video quality and fidelity.

3. Preliminaries

3.1. Task Definition

For the input frames x^1 and $x^N \in \mathbb{R}^{3 \times H \times W}$, frame interpolation aims to generate a video comprising N frames, denoted as $\mathbf{x} \in \mathbb{R}^{N \times 3 \times H \times W}$, where the first and last frames correspond to the input frames.

3.2. Intermediate Flow from Flow-based VFI

Flow-based methods explicitly estimate the correspondence between the starting and ending frames with respect to the intermediate frame, termed the intermediate flow. The intermediate flow can be obtained either by scaling the optical flow between frames [9, 19] or through direct prediction [10, 41]. In this work, we adopt the prediction-based method EMA-VFI [41], owing to its versatility across various time steps and its task-oriented training [39].

Specifically, given the input frames $x^1, x^N \in \mathbb{R}^{3 \times H \times W}$ as well as the n -th frame x^n to be predicted, the intermediate flow f is computed using a learnable network \mathcal{O} :

$$f_{1 \rightarrow n}, f_{N \rightarrow n}, M^n = \mathcal{O}(x^1, x^N, n). \quad (1)$$

Here, $f_{i \rightarrow n} \in \mathbb{R}^{2 \times H \times W}$ denotes the intermediate flow from the i -th frame x^i to the n -th frame x^n , and $M \in \mathbb{R}^{1 \times H \times W}$ represents the occlusion mask between the two frames at the n -th frame, taking values in the range of $(0, 1)$. Subsequently, we can coarsely estimate the intermediate frame \bar{x}^n as follows:

$$\bar{x}^n = \text{warp}(x^1, f_{1 \rightarrow n}) \odot M^n + \text{warp}(x^N, f_{N \rightarrow n}) \odot (1 - M^n), \quad (2)$$



Figure 3. **Comparison of different methods for approximating intermediate frames.** Linear interpolation merely overlays the input frames, while optical flow often introduces significant artifacts. In contrast, the frames warped through intermediate flow demonstrate superior stability, providing the generative model with robust correspondence information.

where $\text{warp}(x^i, f_{i \rightarrow n})$ denotes the backward warping by $f_{i \rightarrow n}$, and \odot signifies the element-wise multiplication.

3.3. VFI with Diffusion Models

Empowered by large-scale pre-training, video diffusion models [2, 35] exhibit remarkable capabilities in generating videos within complex scenarios. Recent works [3, 33–35] have begun to leverage pre-trained video diffusion models for frame interpolation tasks. In this work, we explore our method based on two generative frame interpolation models, DynamiCrafter [35] and ToonCrafter [34], for real-world and animation scenes respectively. Both models are based on Latent Diffusion Models (LDMs) [25], which conduct diffusion in the latent space of an autoencoder. Specifically, for any video $\mathbf{x} \in \mathbb{R}^{N \times 3 \times H \times W}$, where N denotes the number of frames, the video is transformed into the latent space using a pre-trained encoder \mathcal{E} (i.e., VQ-VAE) [25] to obtain the corresponding latent code $\mathbf{z}_0 = \mathcal{E}(\mathbf{x}) \in \mathbb{R}^{N \times C \times h \times w}$.

During training, \mathbf{z}_0 is first converted into an intermediate noisy video at timestep t using the equation:

$$\mathbf{z}_t = \alpha_t \mathbf{z}_0 + \sqrt{1 - \alpha_t} \epsilon, \quad \epsilon \sim \mathcal{N}(0, I). \quad (3)$$

To achieve frame interpolation task, a learnable denoising network ϵ_θ is then employed to predict the noise ϵ given the condition information from the first and the last frames. DynamiCrafter and ToonCrafter incorporate such condition information by:

$$\tilde{\mathbf{z}}_t = [\mathbf{z}_t; \bar{\mathbf{z}}_0], \quad \tilde{\mathbf{z}}_t \in \mathbb{R}^{N \times (2 \times C) \times h \times w}, \quad (4)$$

where $\bar{\mathbf{z}}_0$ is composed of the latent codes of bound frames z_0^1, z_0^N , while other positions remain zero. Then the denoising network is optimized by minimizing the following loss:

$$\mathcal{L}(\theta) = \mathbb{E}_{\mathbf{z}_0, t, \epsilon \sim \mathcal{N}(0, I)} \left[\|\epsilon - \epsilon_\theta(\tilde{\mathbf{z}}_t; t, c)\|_2^2 \right]. \quad (5)$$

Here, c includes other condition information like the text and the fps. After training, we can iteratively recover $\hat{\mathbf{z}}_0$

using the input conditions and pure noise $\mathbf{z}_T \sim \mathcal{N}(0, I)$, generating the video $\hat{\mathbf{x}} = \mathcal{D}(\hat{\mathbf{z}}_0)$ via the decoder \mathcal{D} .

The design of the denoising network ϵ_θ follows an U-Net-like structure [26], consisting of contracting blocks, middle blocks, and expansive blocks. Each block comprises spatial and temporal layers. The spatial layers mainly consist of ResNet blocks [6] and Transformer blocks [31] with spatial attention, modeling spatial information within each frame, while the temporal layers are formed by Transformer blocks with temporal self-attention.

4. Motion-Aware Generative VFI

Currently, most generative interpolation methods [3, 5, 33–35] conduct frame interpolation by directly incorporating information from the input frames into the model’s input [5, 35] or decoder [35]. However, in these methods, the correspondence between input frames, which is crucial for understanding and reasoning about the motion and appearance of the intermediate frames, have to be inferred independently by the generative model itself. This correspondence estimation capability has not been adequately cultivated in the pre-training of large-scale text-to-video generation or pure video generation tasks. Consequently, this insufficient exploration of correspondence leads to inconsistencies in motion and appearance of the generated videos relative to the input frames.

To address this issue, we propose Motion-Aware Generative Frame Interpolation (MoG), the first approach to explicitly introduce correspondence information between the two frames into the generative model, thereby reducing the difficulty of the inference for motion and appearance for generative model. As illustrated in Fig. 2, MoG comprises two parts: it first extracts an explicit motion guidance based on the input frames by a pre-trained flow-based VFI model [41]; it then seamlessly injects this guidance into the generative model at both the latent and feature levels. Notably, our method does not require any additional param-

eters; it merely necessitates minimal fine-tuning steps on spatial layers of the denoising network to compensate for changes in feature distribution.

4.1. Choice of motion guidance

As illustrated in Fig. 3, in addition to the intermediate flow described in Eq. (1), there are two other guidance for representing intermediate frames based on input frames. The first method is linear interpolation, which directly weights the representations of the initial and final frames according to the time step of the intermediate frame. While straightforward, this technique merely overlays the input frames, offering limited correspondence information. The second method employs a pre-trained optical flow estimator, such as [37], to derive the flow between input frames, which is then scaled to generate the intermediate flow. This approach often suffers from limited generalization due to being predominantly trained on synthetic datasets. Moreover, it cannot account for occlusion relationships between input frames. This can lead to artifacts in complex scenes, such as jagged edges and ghosting effects.

In contrast, the intermediate flow defined in Eq. (1) is specifically trained for the VFI task, making it inherently more suitable for representing the correlation between intermediate frames and the initial and final frames. It also predicts an occlusion mask M^n for each frame. As illustrated in Fig. 3, the intermediate flow allows for the approximation of intermediate frames, which, despite some blurriness, maintains stable motion trajectories and consistent object appearances. This stability alleviates the difficulties of real motion inference in generative models. This is further validated by our experiments in Sec. 5.4.

4.2. Motion Guidance Integration

Due to the inability of diffusion models to directly use correspondence guidance, it is necessary to devise a strategy to inject these motion information into the denoising network. To achieve this, we propose a simple yet effective approach that leverages the guidance, akin to the Eq. (2), to coarsely estimate the representation of the intermediate frames from the representations of the start and end frames. This estimated representation is then seamlessly merged into the denoising network. Furthermore, to fully exploit the correspondence guidance across different granularities of the generation process, we conduct the guidance injection at both the latent and feature levels.

Latent-Level Injection. To introduce motion guidance at the latent level, we propose to coarsely estimate the latent code of intermediate frames by backward warping of the input frame’s latent code with the intermediate flow. Specifically, given the latent codes of the start and end frames z_0^1 and z_0^N , along with the motion guidance obtained

via Eq. (1), we estimate the latent code of the n -th intermediate frame:

$$\bar{z}_0^n = \text{warp}(z_0^1, f_{1 \rightarrow n}) \odot M^n + \text{warp}(z_0^N, f_{N \rightarrow n}) \odot (1 - M^n). \quad (6)$$

Here, \bar{z}_0^n represents the estimated latent code for the n -th frame using the motion guidance. During training, the input to the denoising network is modified to:

$$\tilde{\mathbf{z}}_t = [\mathbf{z}_t; \bar{\mathbf{z}}_0], \quad \tilde{\mathbf{z}}_t \in \mathbb{R}^{N \times (2 \times C) \times h \times w}. \quad (7)$$

It is noteworthy that no additional parameters are required, as our base models, DynamiCrafter or ToonCrafter, have already designed to accommodate extra inputs; however, the latent codes of intermediate frames in $\bar{\mathbf{z}}_0$ are always zero at their methods.

Feature-Level Injection. To effectively integrate the motion guidance in different granularities, we propose to inject guidance also in feature-level. Analogous to the latent-level, we estimate the features of intermediate frames based on the features $F^0, F^N \in \mathbb{R}^{D \times H \times W}$ of the input frames:

$$\bar{F}^i = \text{warp}(F^1, f_{1 \rightarrow i}) \odot M^n + \text{warp}(F^N, f_{N \rightarrow i}) \odot (1 - M^n). \quad (8)$$

In this equation, \bar{F}^i represents the estimated features of the i -th frame under the correspondence prior. Unfortunately, unlike in latent-level injection, direct concatenation of the warped intermediate features into the network is not feasible. To address this issue, we leverage the temporal layer of the denoising network, which enables us to smooth and align the estimated intermediate features with the original feature distribution without introducing additional parameters, as shown in Fig. 2:

$$\hat{\mathbf{F}} = \text{Temporal layer}(\bar{\mathbf{F}}). \quad (9)$$

Subsequently, we incorporate the smoothed features $\hat{\mathbf{F}}$ into the original features:

$$\tilde{\mathbf{F}} = (\mathbf{F} + \hat{\mathbf{F}})/2. \quad (10)$$

Remarkably, our exploration (refer to Sec. 5.4) reveals that this simple averaging already allows the generative model to effectively utilize the introduced motion guidance.

5. Experiment

5.1. Implementation Details

We develop MoG based on DynamiCrafter [35] for real-world scenes and ToonCrafter [34] for animation scenes. MoG employs EMA-VFI [41] for intermediate flow prediction. For model fine-tuning, we only train the spatial layers, while keeping all other parameters fixed. We train with the same loss in Eq. (5) for 20K steps on 1×10^{-5} learning rate and batch size 32. The training dataset is internal collected of 512×320 resolution with 16 frames. The sampling strategy is consistent with [35] and [34].

Models	Subject Consistency		Background Consistency		Temporal Flickering		Motion Smoothness		Aesthetic Quality		Imaging Quality		Average	
	Real	Anime	Real	Anime	Real	Anime	Real	Anime	Real	Anime	Real	Anime	Real	Anime
<i>Flow-based VFI models</i>														
RIFE [10]	86.63	86.92	91.67	94.25	97.92	98.46	99.28	99.38	45.18	48.22	46.15	48.11	77.81	79.22
EMA-VFI [41]	87.85	88.97	91.91	95.12	97.39	98.29	99.11	99.29	46.68	50.20	47.96	52.24	78.48	80.69
<i>Generative VFI models</i>														
GI [33]	91.81	91.28	91.70	94.16	93.86	96.43	97.51	98.00	47.44	51.13	57.51	60.84	79.97	81.97
TRF [3]	89.25	89.25	92.26	94.01	93.48	95.77	96.77	97.18	47.94	50.12	54.38	58.40	79.01	80.79
DynamiCrafter [35]	89.06	–	91.94	–	92.97	–	96.39	–	48.47	–	58.24	–	79.51	–
ToonCrafter [34]	–	91.78	–	95.42	–	95.63	–	96.75	–	51.44	–	64.37	–	82.57
MoG (ours)	92.65	92.91	94.34	96.11	94.69	96.58	97.90	96.94	49.84	52.43	59.23	64.89	81.44	83.31

Table 1. **Quantitative comparison on video quality.** Bold text indicates the best results in generative frame interpolation.

Models	PSNR (\uparrow)		SSIM (\uparrow)		LPIPS (\downarrow)		FVD (\downarrow)		FID (\downarrow)		CLIP _{sim} (\uparrow)	
	Real	Anime	Real	Anime	Real	Anime	Real	Anime	Real	Anime	Real	Anime
<i>Flow-based VFI models</i>												
RIFE [10]	18.13	20.27	0.6094	0.7817	0.3745	0.3407	898.38	647.49	65.04	66.16	0.8228	0.8643
EMA-VFI [41]	18.11	20.45	0.6118	0.7843	0.3763	0.3701	808.54	544.48	60.28	55.84	0.8363	0.8895
<i>Generative VFI models</i>												
GI [33]	15.95	18.04	0.5271	0.6971	0.3384	0.2891	521.00	449.31	36.06	46.18	0.8703	0.8710
TRF [3]	15.43	16.49	0.5132	0.6744	0.3920	0.3470	624.63	481.02	42.48	53.95	0.8491	0.8731
DynamiCrafter [35]	16.05	–	0.5225	–	0.3380	–	562.34	–	42.16	–	0.8634	–
ToonCrafter [34]	–	18.01	–	0.7182	–	0.2944	–	425.71	–	40.63	–	0.9203
MoG (ours)	17.82	19.44	0.5898	0.7434	0.2716	0.2615	401.49	351.41	31.26	33.73	0.9083	0.9320

Table 2. **Quantitative comparison on generation fidelity to the ground truth.**

5.2. VFIBench

To evaluate interpolated frames, we present VFIBench, a comprehensive benchmark that encompasses diverse data, including real-world videos and animations. It employs various metrics for a detailed assessment of frame quality and fidelity to ground truth. VFIBench also poses a challenge by requiring models to interpolate 14 frames between specified start and end frames. This setup demands advanced motion modeling capabilities. For data collection, we meticulously selected 100 samples from the DAVIS 2017 dataset [23], referred to as the VFIBench-Real, to reflect real-world scenarios. Additionally, we curate another set of 100 samples from internet animations, called VFIBench-Ani, which includes a diverse range of styles from Japanese, American, and Chinese animations.

A well-interpolated video should not only be of high quality inherently but also maintain fidelity to the ground truth. For the former, we utilize six metrics from VBench [11]: subject consistency, background consistency, temporal flickering, motion smoothness, aesthetic quality, and imaging quality. These metrics collectively assess the intrinsic quality of the video. For the latter, we employ six widely adopted metrics: PSNR, SSIM, LPIPS [43], FID [7], and the CLIP similarity score [24] for image-level comparison, and FVD [29, 30] for video-level comparison.

5.3. Comparative Analysis

We evaluate our MoG by benchmarking it against state-of-the-art methods across two categories: flow-based interpolation methods, specifically RIFE [10] and EMA-VFI [41], and generative interpolation methods, including GI [33], TRF [3], DynamiCrafter [35] and ToonCrafter [34]. Note that DynamiCrafter and ToonCrafter are tailored for real-world and cartoon animation data, respectively, and their performance is reported separately for each data type.

Quantitative results. As shown in Tab. 1 and Tab. 2, compared to others generative VFI methods, MoG exhibits significant improvements in video quality and fidelity to ground truth, particularly in consistency-related metrics. This demonstrates that the introduced motion guidance indeed enables the generative model to better understand the correspondence between input frames. Compared to flow-based VFI models, our approach also demonstrates notable enhancements across most metrics; however, it lags in PSNR, SSIM, Temporal Flickering, and Motion Smoothness. We argue that this discrepancy arises because flow-based VFI often produces blurry results in complex motion scenarios (as illustrated in Fig. 1), which can inflate these metrics while compromising actual visual quality [43].

Qualitative results. We present qualitative comparisons with three generative VFI methods in Fig. 4. Lacking ex-

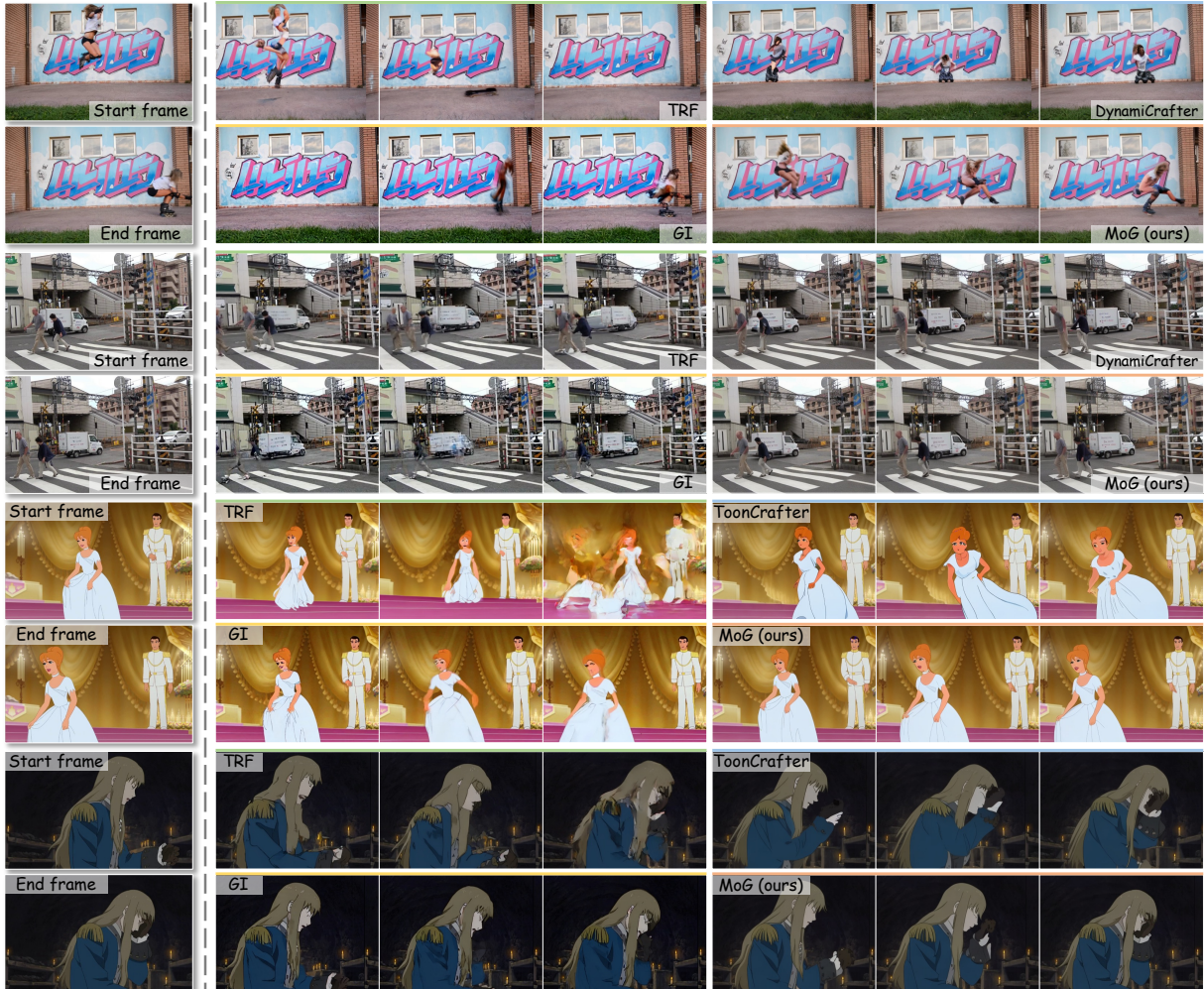


Figure 4. Visual comparison on real-world and animation scenes.

PLICIT motion guidance, these methods struggle to accurately infer and understanding the correspondences between input frames, resulting in inconsistent content and unstable motion. In contrast, MoG achieves superior motion and visual quality in complex scenarios. More comparisons are available on the provided website in supplementary materials.

User study. To further verify the advantage of our method, we also conduct a comprehensive user study. Participants are instructed to select the best-generated videos based on motion quality, temporal coherence, frame fidelity, and overall quality. We collect results from 27 participants and report the findings in Tab. 3. Thanks to the explicit motion guidance, the study shows a clear preference for our method in all aspects.

5.4. Ablation Study

For brevity, we only conduct ablation experiments in real-world scenarios. Our analysis primarily relies on four met-

Methods	Motion Quality	Temporal Coherence	Frame Fidelity	Overall Quality
EMA-VFI [41]	0.49%	0.74%	0.49%	0.49%
TRF [3]	1.73%	1.73%	0.99%	1.48%
GI [33]	16.05%	14.57%	23.21%	15.56%
DynamiCrafter [35]	3.70%	3.21%	4.20%	2.22%
MoG (ours)	78.02%	79.75%	71.11%	80.25%

Table 3. User study statistics.

rics to evaluate different strategies: two pertaining to video quality, namely Subject Consistency and Background Consistency (abbreviated as **Sub. Cons.** and **Bg. Cons.** in Sec. 5.4), and two metrics assessing fidelity between the video and ground truth, specifically LPIPS and FVD.

Effectiveness of motion guidance. As a key contribution of our work, we thoroughly validate the efficacy of the proposed motion guidance. In Fig. 5, (a) displays the results from the DynamiCrafter, which suffers from significant motion instability and content inconsistency. (b) presents out-

	Sub. Cons.	Bg. Cons.	LPIPS	FVD
Only fine-tuning	89.57	92.09	0.3290	540.47
Linear interpolation	90.77	92.75	0.3046	481.41
Pretrained optical flow	91.52	93.44	0.2871	454.29
Flow-based VFI	92.65	94.34	0.2716	401.49

(a) Choice of motion guidance.

	Sub. Cons.	Bg. Cons.	LPIPS	FVD
Transformers	92.35	94.01	0.2750	431.21
Convolution	92.44	94.09	0.2745	426.85
Linear	92.49	94.17	0.2739	422.97
Average	92.65	94.34	0.2716	401.49

(c) Different ways to merge guidance.

Latent	Feature	Sub. Cons.	Bg. Cons.	LPIPS	FVD
		89.57	92.09	0.3290	540.47
✓		91.87	93.92	0.2796	437.85
	✓	92.34	93.74	0.2811	424.50
✓	✓	92.65	94.34	0.2716	401.49

(b) Different levels of guidance injection.

	Sub. Cons.	Bg. Cons.	LPIPS	FVD
All	92.17	93.51	0.2792	451.31
Decoder-only	91.74	92.97	0.2942	471.52
Encoder-only	92.65	94.34	0.2716	401.49

(d) Position of feature-level injection.

Table 4. Ablation experiments. The colored background indicates our default setting.

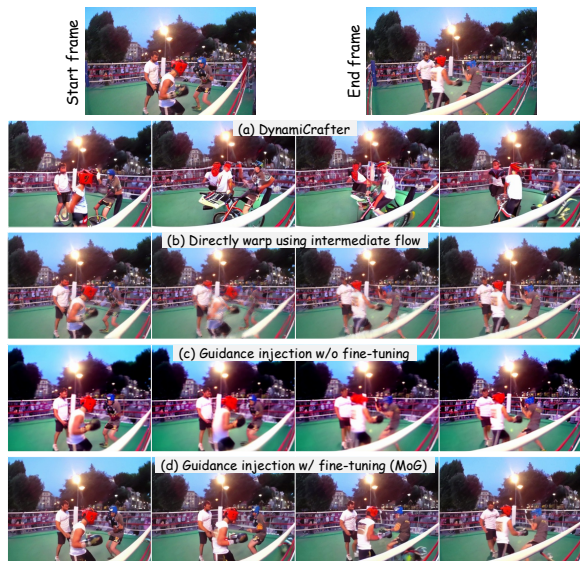


Figure 5. Ablation on motion guidance integration.

comes warped by the intermediate flow from [41]. Although noticeable blurring is evident, the warped intermediate frames offer valuable approximations of both motion and appearance. (c) shows results obtained through direct guidance integration using our method in a train-free manner, demonstrating substantial improvements in motion stabilization. However, this direct integration, lacking training, leads to alterations in feature distribution that affect the color and details of generated frames. Finally, (d) showcases the results of the MoG, which both incorporates guidance and fine-tunes the spatial layers. Our method effectively leverages this guidance, producing realistic motion trajectories and maintaining consistent content. More comparisons can be found in the supplementary materials.

Choice of motion guidance. To select the appropriate motion guidance, we evaluate various approaches in Sec. 4.1 and compare their results with those obtained without motion guidance (only fine-tuning), as shown

in Tab. 4a. As discussed in Sec. 4.1, linear interpolation offers only marginal improvements in video quality and fidelity, whereas the intermediate flow from flow-based VFI achieves superior performance due to its task-oriented training and explicit occlusion modeling.

Different levels of guidance injection. We introduce motion guidance at both the latent and feature levels. To validate the effectiveness of each level, we compare the performance of models with motion guidance introduced at only one level, or without motion guidance, as in Tab. 4d. The results demonstrate that the injection of either level all significantly enhances video quality and fidelity metrics. Specifically, latent-level injection is more beneficial for background consistency, while feature-level injection improves subject consistency. The best performance is achieved when both levels are employed, allowing the generative model to leverage motion guidance at different granularities to facilitate the generation of intermediate frames.

Design details of feature-level injection. We investigate the details of feature-level injection from two perspectives: how and where to merge motion guidance. Regarding how to merge guidance, we also devise methods that first concatenate the warped intermediate features with the original features, followed by learnable modules such as Transformer blocks, convolutions, or linear layers. Surprisingly, as shown in Tab. 4c, a simple averaging yielded the best performance, possibly due to the substantial data requirements for the learnable modules to achieve strong generalization. In terms of where to merge motion guidance, we experiment with three configurations: injecting into all blocks (All), exclusively into expansive blocks (Decoder-only), and solely into contracting blocks (Encoder-only). As illustrated in Tab. 4b, the Encoder-only achieves the best performance, while Decoder-only results in the poorest performance. This discrepancy may stem from the fact that modifications to the decoder can disrupt the powerful video generation capabilities from pre-training.

6. Conclusion

In this work, we have presented a novel generative frame interpolation framework, MoG, which enhances the model’s motion awareness by explicitly incorporating additional motion guidance. We first reveal that the intermediate flow in flow-based VFI can serve as a suitable motion guidance. Subsequently, we propose a simple yet effective strategy to inject this guidance into the generative network at both the latent and feature levels, significantly reducing the challenge of inferring the motion of input frames. Through extensive experiments in both real-world and animated scenes, we demonstrate that MoG achieves substantial improvements in video quality and fidelity. User studies further indicate that MoG exhibits superior overall visual quality.

Appendix

A. More Visual Comparisons

To further demonstrate the improvement of our method, we **provide video comparisons of different methods on the provided website**. We also provide additional qualitative comparisons in Fig. 8.

B. Effectiveness of Introducing Motion Guidance

As shown in Fig. 6, we provide more examples similar to Fig. 5 to demonstrate the effectiveness of introducing motion guidance. By explicitly incorporating a rough estimate of the motion between input frames, our method effectively stabilizes the generated motion and reduces the inconsistency in content between the generated video and the input frames.

C. Discussion on Ineffective Motion Guidance

Our method significantly enhances video generation quality primarily by leveraging the coarse intermediate frame estimates provided by motion guidance. To present a comprehensive analysis, it is essential to demonstrate our method’s performance in scenarios where motion guidance is ineffective. As illustrated in the two examples in Fig. 7, when the motion in the input frames is overly complex, the intermediate flow fails to deliver effective motion guidance. Notably, despite the ineffectiveness of motion guidance in these cases, our approach still yields high-quality results. This indicates that our method, MoG, does not rely entirely on motion guidance for generating identical motion. Instead, it dynamically integrates the effective information from motion guidance to assist in the inference of real motion. This aligns perfectly with our original intent.

D. Limitations and Future Work

Despite MoG has achieved non-trivial improvement in generation quality across various scenes, there still several limitations warrant further exploration. Firstly, our approach

is built upon the U-Net architecture of the DynamiCrafter model. However, the video generation capabilities of DynamiCrafter has lagged behind recently DiT-based [22] video generation models [4, 40], which constrains our performance ceiling. Investigating our method within the new framework presents a promising avenue for future work. Secondly, our approach relies on a pre-trained flow-based VFI model, meaning that the quality of its outputs may impact the effectiveness of motion guidance. For instance, flow-based VFI struggles to establish correspondences for extremely large motion [15]. Enhancing the generalizability of flow-based VFI across diverse scenes will also benefit our method moving forward.

References

- [1] Wenbo Bao, Wei-Sheng Lai, Chao Ma, Xiaoyun Zhang, Zhiyong Gao, and Ming-Hsuan Yang. Depth-aware video frame interpolation. In *Proceedings of the IEEE/CVF conference on computer vision and pattern recognition*, pages 3703–3712, 2019. 2
- [2] Andreas Blattmann, Tim Dockhorn, Sumith Kulal, Daniel Mendelevitch, Maciej Kilian, Dominik Lorenz, Yam Levi, Zion English, Vikram Voleti, Adam Letts, et al. Stable video diffusion: Scaling latent video diffusion models to large datasets. *arXiv preprint arXiv:2311.15127*, 2023. 2, 3, 4
- [3] Haiwen Feng, Zheng Ding, Zhihao Xia, Simon Niklaus, Victoria Abrevaya, Michael J Black, and Xuaner Zhang. Explorative inbetweening of time and space. In *European Conference on Computer Vision*, pages 378–395. Springer, 2025. 2, 3, 4, 6, 7
- [4] Genmo. Mochi 1: A new sota in open-source video generation models. <https://www.genmo.ai/blog>, 2024. 9
- [5] Yuwei Guo, Ceyuan Yang, Anyi Rao, Maneesh Agrawala, Dahua Lin, and Bo Dai. Sparsectrl: Adding sparse controls to text-to-video diffusion models. In *European Conference on Computer Vision*, pages 330–348. Springer, 2025. 4
- [6] Kaiming He, Xiangyu Zhang, Shaoqing Ren, and Jian Sun. Deep residual learning for image recognition. In *Proceedings of the IEEE/CVF Conference on Computer Vision and Pattern Recognition*, pages 770–778, 2016. 4
- [7] Martin Heusel, Hubert Ramsauer, Thomas Unterthiner, Bernhard Nessler, and Sepp Hochreiter. Gans trained by a two time-scale update rule converge to a local nash equilibrium. *Advances in Neural Information Processing Systems*, 30, 2017. 6
- [8] Jonathan Ho, Ajay Jain, and Pieter Abbeel. Denoising diffusion probabilistic models. *Advances in Neural Information Processing Systems*, 33:6840–6851, 2020. 2
- [9] Ping Hu, Simon Niklaus, Stan Sclaroff, and Kate Saenko. Many-to-many splatting for efficient video frame interpolation. In *Proceedings of the IEEE/CVF Conference on Computer Vision and Pattern Recognition*, pages 3553–3562, 2022. 2, 3
- [10] Zhewei Huang, Tianyuan Zhang, Wen Heng, Boxin Shi, and Shuchang Zhou. Real-time intermediate flow estimation for

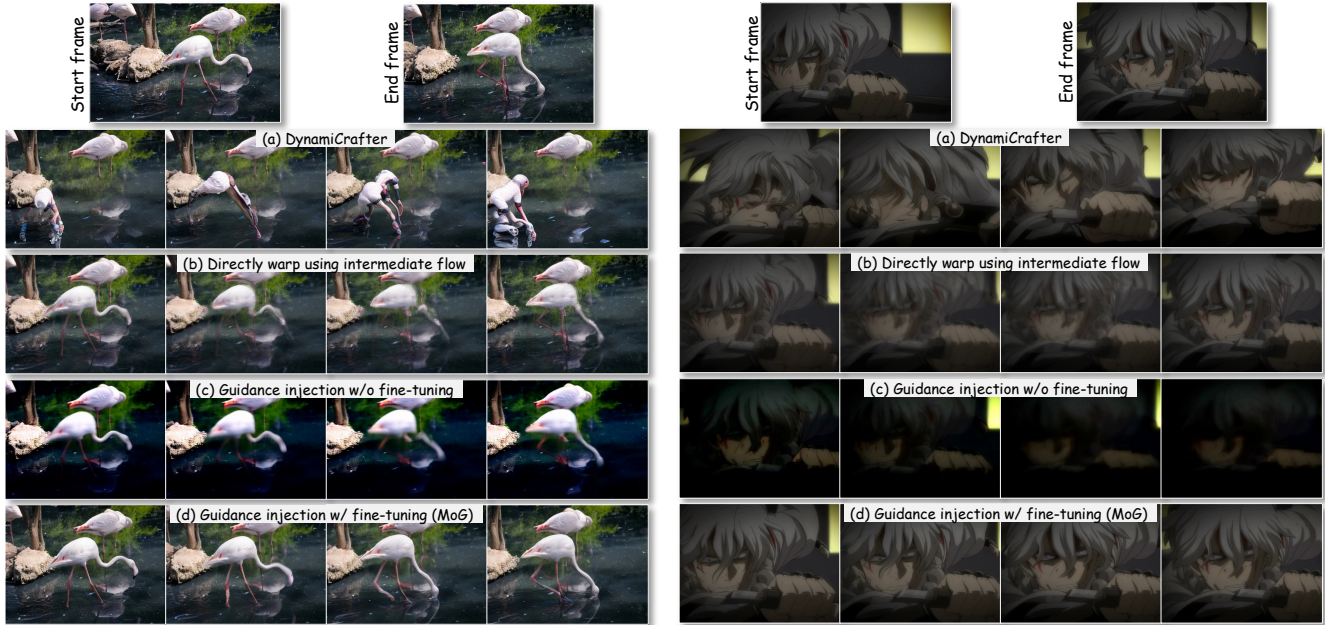


Figure 6. Additional ablation experiments on motion guidance integration.

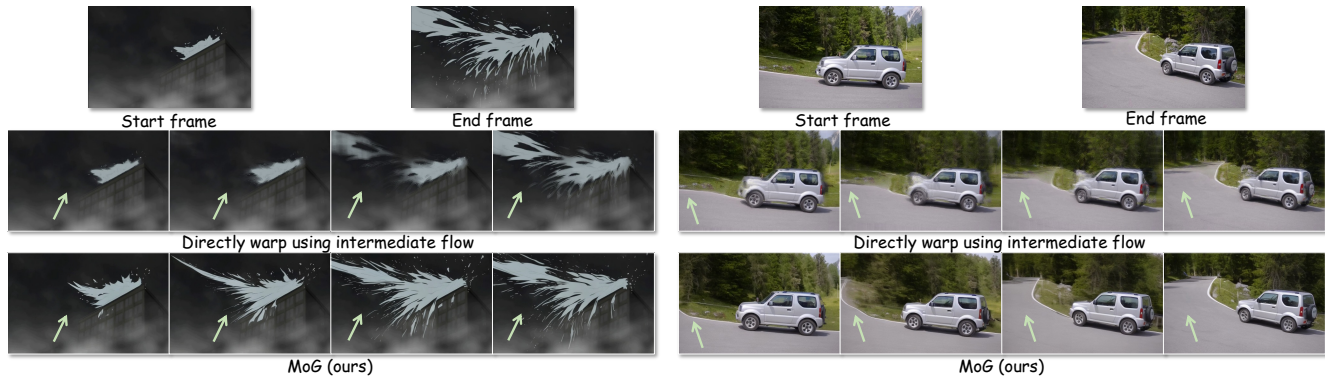


Figure 7. Instances of ineffective guidance.

- video frame interpolation. In *European Conference on Computer Vision*, 2022. 2, 3, 6
- [11] Ziqi Huang, Yanan He, Jiashuo Yu, Fan Zhang, Chenyang Si, Yuming Jiang, Yuanhan Zhang, Tianxing Wu, Qingyang Jin, Nattapol Chanpaisit, et al. Vbench: Comprehensive benchmark suite for video generative models. In *Proceedings of the IEEE/CVF Conference on Computer Vision and Pattern Recognition*, pages 21807–21818, 2024. 6
- [12] Huaizu Jiang, Deqing Sun, Varun Jampani, Ming-Hsuan Yang, Erik Learned-Miller, and Jan Kautz. Super slo-mo: High quality estimation of multiple intermediate frames for video interpolation. In *Proceedings of the IEEE/CVF Conference on Computer Vision and Pattern Recognition*, pages 9000–9008, 2018. 2
- [13] Lingtong Kong, Boyuan Jiang, Donghao Luo, Wenqing Chu, Xiaoming Huang, Ying Tai, Chengjie Wang, and Jie Yang. Ifrnet: Intermediate feature refine network for efficient frame interpolation. In *Proceedings of the IEEE/CVF Conference on Computer Vision and Pattern Recognition*, pages 1969–1978, 2022. 2, 3
- [14] Zhen Li, Zuo-Liang Zhu, Ling-Hao Han, Qibin Hou, Chun-Le Guo, and Ming-Ming Cheng. Amt: All-pairs multi-field transforms for efficient frame interpolation. In *Proceedings of the IEEE/CVF Conference on Computer Vision and Pattern Recognition*, pages 9801–9810, 2023.
- [15] Chunxu Liu, Guozhen Zhang, Rui Zhao, and Limin Wang. Sparse global matching for video frame interpolation with large motion. In *Proceedings of the IEEE/CVF Conference on Computer Vision and Pattern Recognition*, pages 19125–19134, 2024. 2, 3, 9
- [16] Liying Lu, Ruizheng Wu, Huaijia Lin, Jiangbo Lu, and Jiaya Jia. Video frame interpolation with transformer. In *Proceedings of the IEEE/CVF Conference on Computer Vision and Pattern Recognition*, pages 3532–3542, 2022. 3

- [17] Ruibo Ming, Zhewei Huang, Zhuoxuan Ju, Jianming Hu, Lihui Peng, and Shuchang Zhou. A survey on video prediction: From deterministic to generative approaches. *arXiv preprint arXiv:2401.14718*, 2024. 2
- [18] Simon Niklaus and Feng Liu. Context-aware synthesis for video frame interpolation. In *Proceedings of the IEEE/CVF Conference on Computer Vision and Pattern Recognition*, pages 1701–1710, 2018. 2
- [19] Simon Niklaus and Feng Liu. Softmax splatting for video frame interpolation. In *Proceedings of the IEEE/CVF Conference on Computer Vision and Pattern Recognition*, pages 5437–5446, 2020. 2, 3
- [20] Simon Niklaus, Ping Hu, and Jiawen Chen. Splatting-based synthesis for video frame interpolation. In *Proceedings of the IEEE/CVF Winter Conference on Applications of Computer Vision*, pages 713–723, 2023. 2
- [21] Junheum Park, Jintae Kim, and Chang-Su Kim. Biformer: Learning bilateral motion estimation via bilateral transformer for 4k video frame interpolation. In *Proceedings of the IEEE/CVF Conference on Computer Vision and Pattern Recognition*, pages 1568–1577, 2023. 3
- [22] William Peebles and Saining Xie. Scalable diffusion models with transformers. In *Proceedings of the IEEE/CVF International Conference on Computer Vision*, pages 4195–4205, 2023. 9
- [23] Jordi Pont-Tuset, Federico Perazzi, Sergi Caelles, Pablo Arbeláez, Alex Sorkine-Hornung, and Luc Van Gool. The 2017 davis challenge on video object segmentation. *arXiv preprint arXiv:1704.00675*, 2017. 6
- [24] Alec Radford, Jong Wook Kim, Chris Hallacy, Aditya Ramesh, Gabriel Goh, Sandhini Agarwal, Girish Sastry, Amanda Askell, Pamela Mishkin, Jack Clark, et al. Learning transferable visual models from natural language supervision. In *International Conference on Machine Learning*, pages 8748–8763. PMLR, 2021. 6
- [25] Robin Rombach, Andreas Blattmann, Dominik Lorenz, Patrick Esser, and Björn Ommer. High-resolution image synthesis with latent diffusion models. In *Proceedings of the IEEE/CVF Conference on Computer Vision and Pattern Recognition*, pages 10684–10695, 2022. 4
- [26] Olaf Ronneberger, Philipp Fischer, and Thomas Brox. U-net: Convolutional networks for biomedical image segmentation. In *Medical image computing and computer-assisted intervention—MICCAI 2015: 18th international conference, Munich, Germany, October 5-9, 2015, proceedings, part III 18*, pages 234–241. Springer, 2015. 4
- [27] Deqing Sun, Xiaodong Yang, Ming-Yu Liu, and Jan Kautz. Pwc-net: Cnns for optical flow using pyramid, warping, and cost volume. In *Proceedings of the IEEE/CVF Conference on Computer Vision and Pattern Recognition*, pages 8934–8943, 2018. 2
- [28] Zachary Teed and Jia Deng. Raft: Recurrent all-pairs field transforms for optical flow. In *European Conference on Computer Vision*, pages 402–419. Springer, 2020. 2
- [29] Thomas Unterthiner, Sjoerd Van Steenkiste, Karol Kurach, Raphaël Marinier, Marcin Michalski, and Sylvain Gelly. Towards accurate generative models of video: A new metric & challenges. *arXiv preprint arXiv:1812.01717*, 2018. 6
- [30] Thomas Unterthiner, Sjoerd van Steenkiste, Karol Kurach, Raphaël Marinier, Marcin Michalski, and Sylvain Gelly. Fvd: A new metric for video generation. 2019. 6
- [31] A Vaswani. Attention is all you need. *Advances in Neural Information Processing Systems*, 2017. 4
- [32] Vikram Voleti, Alexia Jolicoeur-Martineau, and Chris Pal. Mcvd-masked conditional video diffusion for prediction, generation, and interpolation. *Advances in Neural Information Processing Systems*, 35:23371–23385, 2022. 3
- [33] Xiaojuan Wang, Boyang Zhou, Brian Curless, Ira Kemelmacher-Shlizerman, Aleksander Holynski, and Steven M Seitz. Generative inbetweening: Adapting image-to-video models for keyframe interpolation. *arXiv preprint arXiv:2408.15239*, 2024. 2, 3, 4, 6, 7
- [34] Jinbo Xing, Hanyuan Liu, Menghan Xia, Yong Zhang, Xintao Wang, Ying Shan, and Tien-Tsin Wong. Toon-crafter: Generative cartoon interpolation. *arXiv preprint arXiv:2405.17933*, 2024. 2, 3, 4, 5, 6
- [35] Jinbo Xing, Menghan Xia, Yong Zhang, Haoxin Chen, Wangbo Yu, Hanyuan Liu, Gongye Liu, Xintao Wang, Ying Shan, and Tien-Tsin Wong. Dynamicrafter: Animating open-domain images with video diffusion priors. In *European Conference on Computer Vision*, pages 399–417. Springer, 2025. 2, 3, 4, 5, 6, 7
- [36] Haofei Xu, Jing Zhang, Jianfei Cai, Hamid Rezafofighi, and Dacheng Tao. Gmflow: Learning optical flow via global matching. In *Proceedings of the IEEE/CVF Conference on Computer Vision and Pattern Recognition*, pages 8121–8130, 2022. 2
- [37] Haofei Xu, Jing Zhang, Jianfei Cai, Hamid Rezafofighi, Fisher Yu, Dacheng Tao, and Andreas Geiger. Unifying flow, stereo and depth estimation. *IEEE Transactions on Pattern Analysis and Machine Intelligence*, 2023. 2, 5
- [38] Tianfan Xue, Baian Chen, Jiajun Wu, Donglai Wei, and William T Freeman. Video enhancement with task-oriented flow. *International Journal of Computer Vision*, 127:1106–1125, 2019. 2
- [39] Tianfan Xue, Baian Chen, Jiajun Wu, Donglai Wei, and William T Freeman. Video enhancement with task-oriented flow. *International Journal of Computer Vision*, 127:1106–1125, 2019. 3
- [40] Zhuoyi Yang, Jiayan Teng, Wendi Zheng, Ming Ding, Shiyu Huang, Jiazheng Xu, Yuanming Yang, Wenyi Hong, Xiaohan Zhang, Guanyu Feng, et al. Cogvideox: Text-to-video diffusion models with an expert transformer. *arXiv preprint arXiv:2408.06072*, 2024. 9
- [41] Guozhen Zhang, Yuhan Zhu, Haonan Wang, Youxin Chen, Gangshan Wu, and Limin Wang. Extracting motion and appearance via inter-frame attention for efficient video frame interpolation. In *Proceedings of the IEEE/CVF Conference on Computer Vision and Pattern Recognition*, pages 5682–5692, 2023. 2, 3, 4, 5, 6, 7, 8
- [42] Guozhen Zhang, Chunxu Liu, Yutao Cui, Xiaotong Zhao, Kai Ma, and Limin Wang. Vfimbamba: Video frame interpolation with state space models. In *Advances in Neural Information Processing Systems*, 2024. 2, 3
- [43] Richard Zhang, Phillip Isola, Alexei A Efros, Eli Shechtman, and Oliver Wang. The unreasonable effectiveness of

deep features as a perceptual metric. In *Proceedings of the IEEE/CVF Conference on Computer Vision and Pattern Recognition*, pages 586–595, 2018. [6](#)

- [44] Yupeng Zhou, Daquan Zhou, Ming-Ming Cheng, Jiashi Feng, and Qibin Hou. Storydiffusion: Consistent self-attention for long-range image and video generation. *arXiv preprint arXiv:2405.01434*, 2024. [3](#)

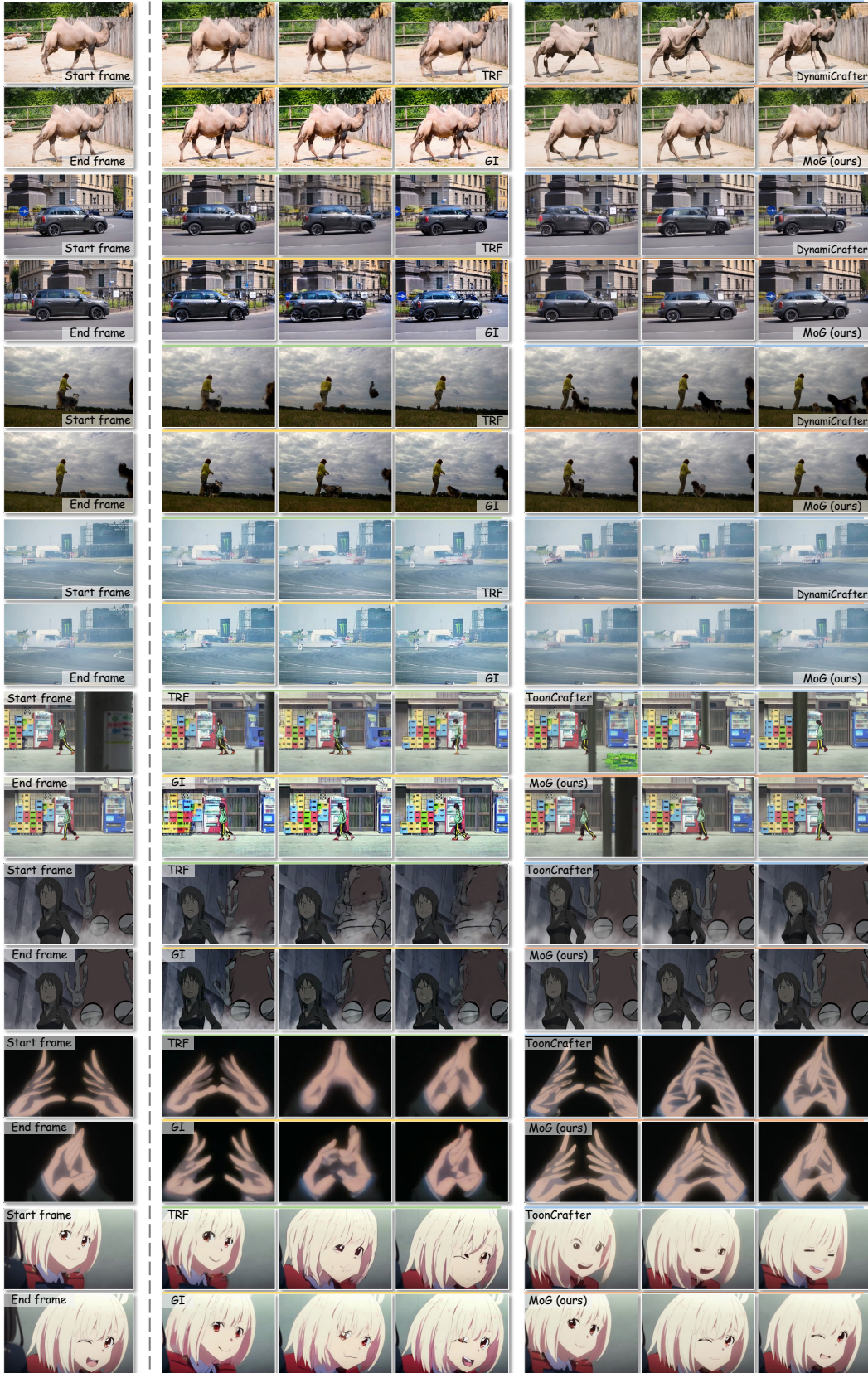


Figure 8. Additional qualitative comparison on real-world and animation scenes.